



# Synthesis and Gas-Sensing Property of Highly Self-assembled Tungsten Oxide Nanosheets

Liangbin Hu, Pengfei Hu, Yong Chen\*, Zehui Lin and Changjun Qiu\*

School of Mechanical Engineering, University of South China, Hengyang, China

We report the synthesis of tungsten oxide ( $\text{WO}_3$ ) nanosheets using a simple yet efficient hydrothermal technique free of surfactant and template. The  $\text{WO}_3$  nano-sheets are self-assembled as well to form ordered one-dimensional chain nanostructure. A comprehensive microscopic characterization reveals that the nano-sheets have triangular and circular two different shape edges, dislocation and stacking faults are also observed, which should have implications for our understanding of catalytic activity of ceria. We also propose a growth mechanism for the nano-sheets. As a result of this unique morphology, this  $\text{WO}_3$  nano-sheets are found to show excellent gas-sensing properties which can use as promising sensor materials detecting ethanol with low concentration.

**Keywords:** crystal structure, defects, nanosheets, highly self-assembled, gas-sensitivity

## OPEN ACCESS

### Edited by:

Zhongchang Wang,  
Laboratório Ibérico Internacional de  
Nanotecnologia (INL), Portugal

### Reviewed by:

Jun Wang,  
Shenzhen University, China  
Xin Wang,  
Shenzhen University, China

### \*Correspondence:

Yong Chen  
chenyongjsnt@163.com  
Changjun Qiu  
qiuchangjun@hotmail.com

### Specialty section:

This article was submitted to  
Nanoscience,  
a section of the journal  
Frontiers in Chemistry

**Received:** 02 June 2018

**Accepted:** 12 September 2018

**Published:** 05 October 2018

### Citation:

Hu L, Hu P, Chen Y, Lin Z and Qiu C  
(2018) Synthesis and Gas-Sensing  
Property of Highly Self-assembled  
Tungsten Oxide Nanosheets.  
*Front. Chem.* 6:452.  
doi: 10.3389/fchem.2018.00452

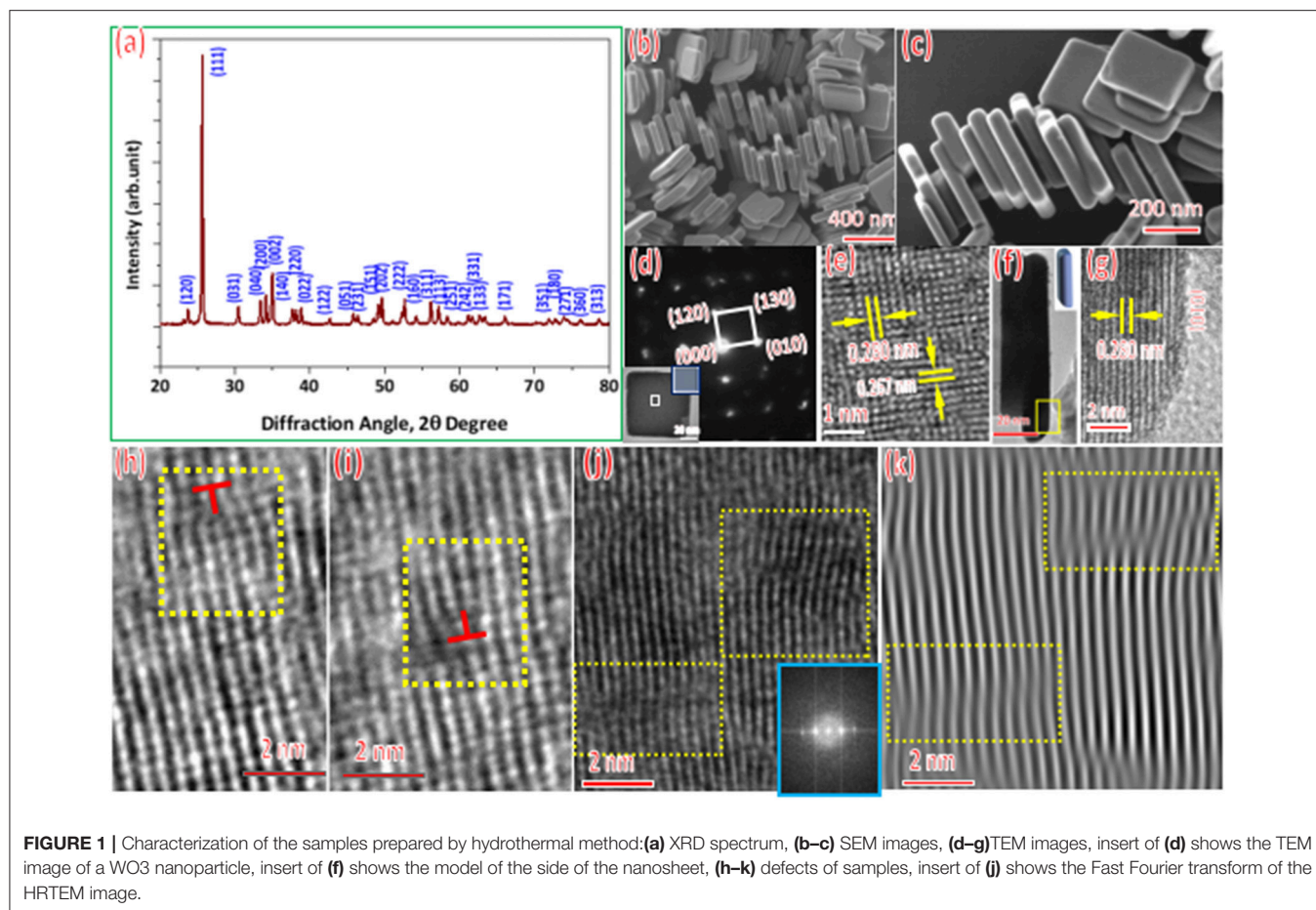
## INTRODUCTION

Tungsten trioxide  $\text{WO}_3$  nanomaterials are extensively applied in electrochromic device, gas sensor and photocatalysts filed (Hai et al., 2016; Zhang et al., 2018). Great effort has been devoted to the control the specific size and shape of  $\text{WO}_3$  nanoparticles which can significantly impact properties of materials. Up to now, the  $\text{WO}_3$  nanoparticles with a variety of morphologies (such as nano-wires, nano-rods, nano-plate, nano-spheres and so on) have been synthesized successfully via high-intensity ultrasound, rapid microwave, hydrothermal synthesis and other methods (Chai et al., 2016; Hu et al., 2017a, Xu et al., 2017; Chen et al., 2018; Parthibavarman et al., 2018; Zhan et al., 2018). Among all of those applied methods, hydrothermal synthesis technique has been concerned due to the merits of simple operation, low energy consumption, the possibility for large-scale industrialization and so on.

Here, we report the  $\text{WO}_3$  nano-sheets with highly self-assembled architecture synthesized via the hydrothermal synthesis process. Defects are observed in the nano-sheets, which may play a key role in affecting properties of  $\text{WO}_3$  nano-sheets. In addition, we also test the response and selectivity of the sensor fabricated from the  $\text{WO}_3$  nano-sheets.

## MATERIALS AND METHODS

All the reagents were analytical grade and without further purification. We adopted a facile hydrothermal method to synthesize the nanostructures. First of all, 32 ml of deionized water and 8 ml glycerol ( $\text{C}_3\text{H}_8\text{O}_3$ ) were mixed into a mixture, then 1.6 nmol of sodium tungstate dihydrate ( $\text{Na}_2\text{WO}_4 \cdot 2\text{H}_2\text{O}$ ) and 3 nmol oleic acid ( $\text{C}_{18}\text{H}_{34}\text{O}_2$ ) were dispersed into the mixture, and stirred for 15 min with a magnetic stirrer. Secondly, the pH of the mixture was adjusted to 1.25 by HCl. After stirring for 15 min, the solution was transferred into the Teflon-lined stainless steel autoclave and treated at  $120^\circ\text{C}$  during 12 h under autogenously pressure.



Finally, the obtained particles were washed by deionized and alcohol to remove the unexpected ions by high-speed centrifugation and then dried at 60°C for 10 h in air.

The characterization of specimen as our previous work (Chen et al., 2013, 2014; Hu et al., 2017b). The process of measuring the gas sensitivity of the prepared nanomaterials is described in the literature (Guo and Wang, 2016). Response of the sensors was defined as the ratio of  $R_a$  (resistances in air) to  $R_g$  (resistances in target gases).

## RESULTS

**Figure 1a** shows a typical XRD spectrum of the products, the diffraction peaks match well with those of a standard WO<sub>3</sub>·H<sub>2</sub>O with orthorhombic structure (JCPDS No. 84-0886). The WO<sub>3</sub>·H<sub>2</sub>O nano-particles exhibit rectangle shape with an average size of ~400 nm and thickness of 30 nm (**Figure 1b**). In addition, one-dimensional chain nanostructure is self-assembled by the quadrilateral faces on the both sides of the nano-sheets. The face of nano-sheet are flat (**Figures 1b,c**). The corresponding SADP identifies that the structure of WO<sub>3</sub> nano-sheets is orthorhombic (**Figures 1d**). **Figure 1e** shows a high-resolution TEM (HRTEM) image taken around the corner of a nano-sheet. We determined the lattice spacing of the perpendicular

lattice fringes to be ~0.280 and ~0.267 nm which are belong to the WO<sub>3</sub> (010) and (120) planes respectively. **Figure 1g** shows a HRTEM image taken from the corner area of the nano-sheet **Figure 1f** from which lattice spacing is determined to be ~0.280 nm, in line with the distance between {010} planes of WO<sub>3</sub>. In addition, the edges of the nano-sheets are in an arc shape (insert of **Figure 1f**). Two different direction edge dislocations: positive edge dislocation (**Figure 1h**) and negative edge dislocation (**Figure 1i**) are detected by the HR-TEM, which should be critical for the properties of WO<sub>3</sub>. Apart from the defects on the surface, we also observed the stacking faults in nano-sheet (**Figure 1j**), which should impact the properties of WO<sub>3</sub> nanoparticles as well. The stacking fault was observed obviously by the one-dimensionally filtered HR-TEM images of the WO<sub>3</sub> nano-sheet (**Figure 1k**). Those dislocations and stacking faults may affect the catalytic activity or other properties of nano material (Wang et al., 2011, 2014, 2016; Sun et al., 2015).

**Figure 2** shows the gases (NH<sub>3</sub>, CH<sub>3</sub>OH, C<sub>6</sub>H<sub>6</sub>) response of the sensor based on WO<sub>3</sub> nanosheets. All of the gases were tested at an operating temperature of 300°C with a concentration of 30 ppm. In **Figure 2**, the results indicate that the sensor exhibited little responses to NH<sub>3</sub>, C<sub>6</sub>H<sub>6</sub>, to indicated that it was insensitive to NH<sub>3</sub>, C<sub>6</sub>H<sub>6</sub>. For ethanol, the highest response of the sensor was 25.6, while the responses to NH<sub>3</sub> and C<sub>6</sub>H<sub>6</sub> were no >1.

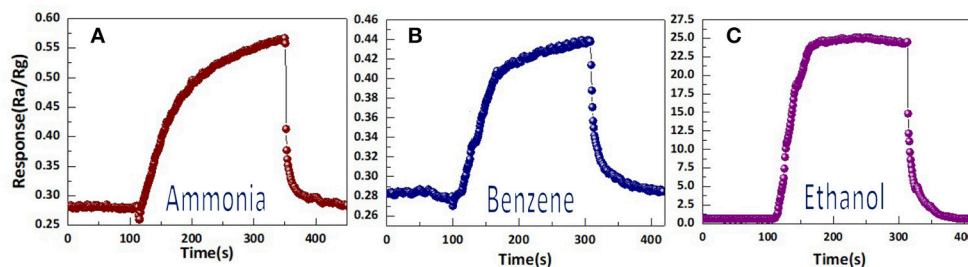
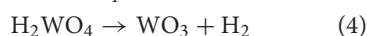
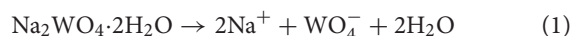


**FIGURE 2** | The response of highly self-assembled tungsten oxide nanosheets sensor toward 30 ppm of different testing gases: (a) ammonia, (b) benzene, (c) ethanol.

## DISCUSSION

In light of the aforementioned microstructural characterization, we propose a likely growth mechanism for the nanosheet. First, the Na<sub>2</sub>WO<sub>4</sub>·2H<sub>2</sub>O is ionized to WO<sub>4</sub><sup>−</sup>. Then, the WO<sub>4</sub><sup>−</sup> ion react with H<sup>+</sup> which ionized by HCl, forming the H<sub>2</sub>WO<sub>4</sub> suspension. The H<sub>2</sub>WO<sub>4</sub> suspension decomposes, at the high temperature and pressure during hydrothermal process, resulting in to the nucleation of WO<sub>3</sub>. The oleic acid acts as a soft template and controls the growth rate of different crystal plane owing to its selective absorption and desorption behavior. Then most of WO<sub>3</sub> nano-sheets with {010} exposure planes are self-assembled, forming one-dimensional chain nanostructures, due to the addition of oleic acid. The formation process can be described as follows:



We imply that the WO<sub>3</sub> nano-sheets can act as an efficient gas-sensing material for selective detection of ethanol. Such the sensing performance due to the fact that the diffusion of ethanol and its oxidation with O<sup>−</sup> or O<sup>2−</sup> are very rapidly in nanoplates structures (Xiao et al., 2017). When sensor prepared by the WO<sub>3</sub> nanosheets is exposed in air, the resistance of the WO<sub>3</sub> nanosheets is increased by oxygen molecules which adsorbed on the surfaces of the WO<sub>3</sub> nanosheets, trapping electrons in the conduction band and forming oxygen species (O<sup>−</sup>, O<sup>2−</sup>). As ethanol is introduced to the sensor, the oxygen species (O<sup>−</sup>, O<sup>2−</sup>) react with ethanol molecules on the surface of the WO<sub>3</sub> nanosheets, which will release trapped electrons to conduction

## REFERENCES

Ahmad, M. Z., Sadek, A. Z., Ou, J. Z., Yaacob, M. H., Latham, K., and Wlodarski, W. (2013). Facile synthesis of nanostructured WO<sub>3</sub> thin films and their characterization for ethanol sensing. *Mater. Chem. Phys.* 141, 912–919. doi: 10.1016/j.matchemphys.2013.06.022

band and resistance of the WO<sub>3</sub> nanosheets is decreased (Ahmad et al., 2013).

## CONCLUSIONS

We have adopted the hydrothermal technique to synthesize highly self-assembled WO<sub>3</sub> nano-sheets using the tungsten resource Na<sub>2</sub>WO<sub>4</sub>·2H<sub>2</sub>O and the soft template oleic acid. We demonstrated that the WO<sub>3</sub> nano-sheets are mainly exposed with {010} planes and crystal defects such as edge dislocations and stacking faults exist in single crystalline nano WO<sub>3</sub> by microscopic investigations, which may be important for the catalytic activity of WO<sub>3</sub>. We indicate that the WO<sub>3</sub> nano-sheets could be used as promising sensor material for detecting CH<sub>3</sub>OH with low concentration.

## AUTHOR CONTRIBUTIONS

LH synthesized and characterized the microstructure of highly self-assembled tungsten oxide nanosheets and wrote the manuscript. PH and ZL tested the response and selectivity of the sensor fabricated from the WO<sub>3</sub> nano-sheets. YC and CQ directed the experiment. All authors read and approved the manuscript.

## ACKNOWLEDGMENTS

YC thanks the financial support by the Construct Program of the Key Discipline of Hunan province (Education Department of Hunan Province Bulletin grant no.[2014]85). ZL thanks the financial support by the Project of Research Study and Creativity Experiment Plan for College Students of the Hunan province (Education Department of Hunan Province Bulletin grant no.[2016]283).

Chai, Y., Ha, F. Y., Yam, F. K., and Hassan, Z. (2016). Fabrication of tungsten oxide nanostructure by sol-gel method. *Proc. Chem.* 19, 113–118. doi: 10.1016/j.proche.2016.03.123

Chen, G. C., Chua, X. F., Qiao, H. B., Ye, M. F., Chen, J., Gao, C., et al. (2018). Thickness controllable single-crystal WO<sub>3</sub> nanosheets: highly selective sensor for triethylamine detection at room temperature. *Mater. Lett.* 226, 59–62. doi: 10.1016/j.matlet.2018.05.022

- Chen, Y., Liu, T. M., Chen, C. L., Guo, W. W., Sun, R., Lv, S., et al. (2013). Synthesis and characterization of CeO<sub>2</sub> Nano-rods. *Ceram. Int.* 39, 6607–6610. doi: 10.1016/j.ceramint.2013.01.096
- Chen, Y., Lv, S. H., Chen, C. L., Qiu, C. J., Fan, X. F., and Wang, Z. C. (2014). Controllable synthesis of ceria nanoparticles with uniform reactive {100} exposure planes. *J. Phys. Chem. C* 118, 4437–4443. doi: 10.1021/jp410625n
- Guo, W. W., and Wang, Z. C. (2016). Composite of ZnO spheres and functionalized SnO<sub>2</sub> nanofibers with an enhanced ethanol gas sensing properties. *Mater. Lett.* 169, 246–249. doi: 10.1016/j.matlet.2016.01.118
- Hai, G., Huang, J., Jie, Y., Li, J., Cao, L., Zhang, G., et al. (2016). Influence of octadecylamine on the phase composition and the photocatalytic property of the tungsten oxide. *Mater. Lett.* 174, 134–137. doi: 10.1016/j.matlet.2016.03.049
- Hu, P. F., Chen, Y., Chen, Y., Lin, Z. H., and Wang, Z. C., (2017a). Hydrothermal synthesis and photocatalytic properties of WO<sub>3</sub> nanorods by using capping agent SnCl<sub>4</sub>·5H<sub>2</sub>O. *Phys. E* 92, 12–16. doi: 10.1016/j.physe.2017.05.004
- Hu, P. F., Chen, Y., Sun, R., Chen, Y., Yin, Y. R., Wang, Z. C., et al. (2017b). Synthesis, characterization and frictional wear behavior of ceria hybrid architectures with {111} exposure planes. *Appl. Surf. Sci.* 401, 100–105. doi: 10.1016/j.apsusc.2017.01.005
- Parthibavarman, M., Karthik, M., and Prabhakaran, S. (2018). Facile and one step synthesis of WO<sub>3</sub> nanorods and nanosheets as an efficient photocatalyst and humidity sensing material. *Vacuum* 155, 224–232. doi: 10.1016/j.vacuum.2018.06.021
- Sun, R., Wang, Z. C., Saito, M., Shibata, N., and Ikuhara, Y. (2015). Atomistic mechanisms of nonstoichiometry-induced twin boundary structural transformation in titanium dioxide. *Nat. Commun.* 6:7120. doi: 10.1038/ncomms8120
- Wang, Z. C., Saito, M., McKenna, K. P., Fukami, S., Sato, H., Ikeda, S., et al. (2016). Atomic-scale structure and local chemistry of CoFeB-MgO magnetic tunnel junctions. *Nano Lett.* 16, 1530–1536. doi: 10.1021/acs.nanolett.5b03627
- Wang, Z. C., Saito, M., McKenna, K. P., Gu, L., Tsukimoto, S., Shluger, A. L., et al. (2011). Atom-resolved imaging of ordered defect superstructures at individual grain boundaries. *Nature* 479, 380–383. doi: 10.1038/nature10593
- Wang, Z. C., Saito, M., McKenna, K. P., and Ikuhara, Y. (2014). Polymorphism of dislocation core structures at the atomic scale. *Nate Commun.* 5:3239 doi: 10.1038/ncomms4239
- Xiao, J., Song, C. W., Dong, W., Chen, L., and Yanyan, Y. (2017). Synthesis, characterization, and gas sensing properties of WO<sub>3</sub> nanoplates. *Rare Metal Mater. Eng.* 46, 1241–1244. doi: 10.1016/S1875-5372(17)30144-3
- Xu, L., Gu, D. X., Chang, X. T., Chai, L. G., Li, Z., Jin, X., et al. (2017). Rare-earth-doped tungsten oxide microspheres with highly enhanced photocatalytic activities. *Ceram. Int.* 43, 10263–10269. doi: 10.1016/j.ceramint.2017.05.055
- Zhan, Y., Liu, Y. L., Liu, Q. Q., Liu, Z. M., Yang, H., Lei, B., et al. (2018). Size-controlled synthesis of fluorescent tungsten oxide quantum dots via one-pot ethanol-thermal strategy for ferric ions detection and bioimaging. *Sens. Actuats B Chem.* 255, 290–298. doi: 10.1016/j.snb.2017.08.043
- Zhang, J., Fu, X., Hao, H., and Gan, W. (2018). Facile synthesis 3D flower-like Ag@WO<sub>3</sub> nanostructures and applications in solar-light photocatalysis. *J. Alloys Compd.* 757, 134–141. doi: 10.1016/j.jallcom.2018.05.068

**Conflict of Interest Statement:** The authors declare that the research was conducted in the absence of any commercial or financial relationships that could be construed as a potential conflict of interest.

Copyright © 2018 Hu, Hu, Chen, Lin and Qiu. This is an open-access article distributed under the terms of the Creative Commons Attribution License (CC BY). The use, distribution or reproduction in other forums is permitted, provided the original author(s) and the copyright owner(s) are credited and that the original publication in this journal is cited, in accordance with accepted academic practice. No use, distribution or reproduction is permitted which does not comply with these terms.